_____

DYNAMIC PROPERTIES OF CABLE-STAYED SYSTEM

Marija Demšić[1*] – Verica Raduka[1] – Kristina Škrtić[2]

[1]Department of Engineering Mechanics, Faculty of Civil Engineering, University of Zagreb, Kačićeva 26, 10000 Zagreb
[2]PhD student, Faculty of Civil Engineering, University of Zagreb, Kačićeva 26, 10000 Zagreb

Abstract:

It is well known that non-linear vibrations of long span cables present a considerable problem of lightweight structures like suspended roofs, cable stayed bridges and cable stayed masts. In the analysis of global structural behaviour, cables are often modelled as equivalent tendon elements. The importance of modelling coupled cable-structure dynamics has been demonstrated by a number of researchers. Dynamic response of non-linear systems can lead to internal or auto-parametric resonance in the case of integer frequency ratio. The analysis of cable-stayed system frequency spectra can show parameter values for which integer frequency ratio condition is fulfilled. In this paper an analytic model of simplified cable-stayed system is formulated. Parabolic cable is modelled using the assumption of quasi-static stretching, while the structure is modelled as Euler-Bernoulli beam. Equations of motions are derived by Hamilton's principle and then linearized around a static equilibrium configuration. Differential equations of motion are solved by the method of variable separation. System deformation is described using analytical functions. Equations of motions together with boundary conditions are solved in closed form to obtain a characteristic equation. For chosen system parameters, the eigenvalue spectra are determined. Parametric analysis of dynamical properties is carried out and integer frequency ratios along with the associated modes are pointed out. Analytic solutions are verified with finite element modelling.

1 Introduction

In modern architecture, cable-supported structures are characterized by a variety of aesthetic shapes that are often accomplished with long span cables.

A cable transfers the load by using tensile force and changes in its geometry. The tensile load transfer ensures a better use of material without the risk of various stability problems and high flexibility makes them quite geometrically non-linear. Because

---

[*] Corresponding author. Tel.: +3851 4639 363 ; fax: +3851 4828 049
E-mail address: mdemsic@grad.hr.

_____

of flexibility, small mass and low damping cables are sensitive to dynamic excitations and are prone to exhibit large amplitude oscillations. Some of the long span cable structures that frequently experience vibration problems caused by dynamic loads (traffic, wind or earthquakes) are cable-stayed bridges. In engineering models, cables are very often treated as equivalent tendon elements and most of studies concerning non-linear behavior of the cables due to static or dynamic actions are carried out on a cable model separated from the structure.

The mathematical model of cable oscillations includes quadratic and cubic nonlinearities resulting from initial cable curvature and stretching. Cubic nonlinearities are more significant and have a great influence on the response of low-sag and highly pretension cables often used as structural elements in civil engineering. Luo *et al.* [1] in their study showed that the dynamic response of multi-degree-of-freedom system with cubic nonlinearities subjected to soft harmonic excitation in the case of well separated natural frequencies is dominated by a primarily excited mode. However, cable structures are specific because of integer ratio of cable natural frequencies and therefore today we have some research concerning non-linear coupling of cable modes. In the research [2], free cable vibrations are analyzed using analytically formulated model and numerical methods. For certain system parameters, the condition of integer frequency ratio is fulfilled and dynamic response can be influenced by internal resonance depending on modes involved in the response and amplitude value. Dynamic excitation of cables can come from various sources like wind, snow, rain or earthquakes, but also cable motion can cause dynamic response of other structural parts. Several studies have shown that external and parametric excitations of the cable are result of small displacement of the support, i.e., connecting joint with the structure [3, 4, 5]. Also, the coupling of primary and parametric resonance is possible in the case of integer frequency ratio [6].

Small scale physical model of cable-stayed bridge was experimentally investigated by Caetano [7]. The research showed that there is considerable dynamic interaction between the cables and the deck/towers. Lin *et al.* [8] analyzed frequencies using a full scale finite element model of cable-stayed bridge and then pointed out that there are several frequencies with integer ratio that include local cable and global modes of the structure. For one-to-one internal resonance case, they formed a simplified analytical model and analyzed reduced system response which showed that large oscillation amplitudes of the cable are induced by dynamic excitation of the beam. Gattulli *et al.* [9] analyzed dynamic properties of a cable-stayed beam and showed that the system has global, local and coupled modes. Also, the frequencies of the local cable and global/coupled system modes in the range of technically relevant parameter values have integer frequency ratio. In a related study [10], the system is reduced on two-degree-of-freedom to analyze non-linear interaction of the cable and the beam. The analysis showed that a small level of dynamic excitation can produce periodic, quasi-periodic and chaotic system response for 2:1 and 1:2 frequency ratios between global and local modes.

In this paper, dynamic properties of a cable-stayed system are analyzed using extended analytic model based on the cable-stay system proposed by Gattulli [9]. Differential equations of motion are derived using the Hamilton's principle. Equations have been expressed in dimensionless form and cable and system parameters have been defined. The method of variable separation was applied to dimensionless equations, assuming continuous functions for system deformation the characteristic equation was obtained in an analytical form. The analysis of dynamic properties is carried out for different cable and system parameters. The verification of the analytic results for certain system parameters is done with the finite element model.

2   Analytical model of continuous system

The model of cable-stayed system is shown in Fig. 1(a). This very simple model is chosen because of its simplicity and possibility to model a system analytically. The interaction between cable and beam is generated through the force and the displacement of the connecting joint. If right conditions for frequency ratio and amplitude value are fulfilled, dynamic response of the beam can excite external and/or parametric oscillations of the cable or cable oscillations can generate the periodic force that is at one end imposed on the beam, also generating external and/or parametric excitation on the beam. The necessary condition for excitation of non-linear auto-parametric oscillations is integer

_____

ratio of system frequencies. Therefore, a detailed analysis of frequency spectra prior to non-linear analysis is required.

Cables with bigger span are usually more prone to the oscillation with large amplitudes. An analytical model analyses only longer cable dynamic, therefore, in order to form even a simpler model, the shorter cable is treated as the massless elastic tendon. Modelling a real cable stay as equivalent tendon is possible by taking into account its elasticity and a variation in its geometry. It can be described as if two springs of elastic and one of geometric stiffness were connected in series. That behavior is often taken into account with tangent modulus of elasticity derived by H.J. Ernest [11]. The dynamic behavior of shorter cable will be neglected and it is replaced with elastic spring in the middle of beam span. We assume small displacement and impose the geometric constraint of the tendon and the beam in node A:

$$\Delta = \delta \sin \gamma, \qquad (1)$$

where Δ is total elongation of the tendon and δ is vertical beam displacement. The tendon geometric stiffness is neglected and equivalent spring stiffness is determined by equating potential energy of the tendon and elastic spring:

$$k = \frac{E_t A_t}{L_t} \sin^2 \gamma. \qquad (2)$$

In expression (2), $E_t A_t$ denote axial tendon stiffness and $L_t = l/(2\cos\gamma)$ its length.

2.1 Equations of motion

According to Hamilton's principle, the governing equations of motion can be obtained by the following equation:

$$\delta \int_{t_1}^{t_2} (T - U) \mathrm{d}t = 0, \qquad (3)$$

where T is kinetic and U total potential energy.

We consider cable and beam to be homogenous one-dimensional elastic continuum, obeying a linear stress-strain relation. We assume an ideally flexible cable and neglect its torsional and shear rigidities. The beam is modeled neglecting its axial, torsional, shear strain and geometric non-linarites. With regard to the static equilibrium position, the potential energy of the system is:
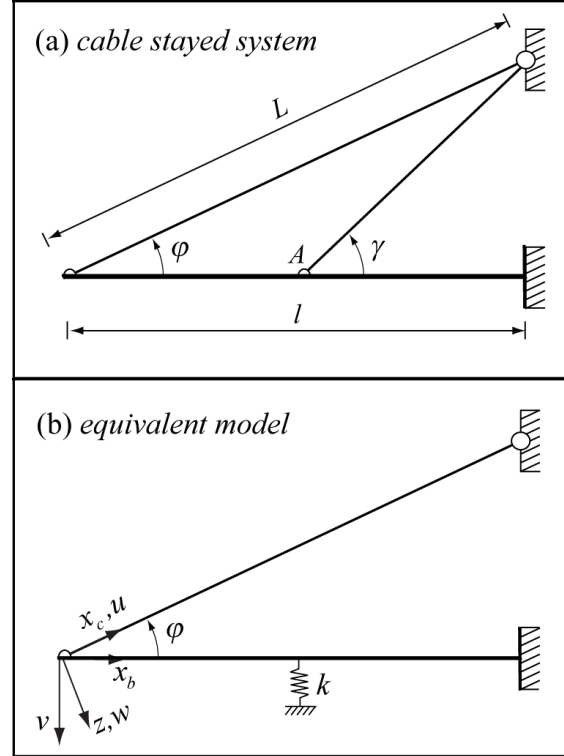

Figure 1. Model of cable-stayed system.

$$U = \tfrac{1}{2} \int_0^l E_b I_b \, \kappa^2 \mathrm{d}x_b + \tfrac{1}{2} \int_0^L E_c A_c \, \varepsilon^2 \mathrm{d}x_c - \int_0^l m_b g \, v \, \mathrm{d}x_b \\ + \int_0^L m_c g \sin\varphi \, u \, \mathrm{d}x_c - \int_0^L m_c g \cos\varphi \, w \, \mathrm{d}x_c. \qquad (4)$$

In the equation (4), the cable longitudinal and transverse components of dynamic displacements are $u(x_c,t)$ and $w(x_c,t)$, respectively. The transverse dynamic displacement of the beam is denoted as $v(x_b,t)$. The first and second term represent potential energy of the beam due to bending and cable elastic strain energy. Remaining terms are gravitational potential energy. Due to static and dynamic actions, beam curvature κ is defined by linear geometric approximation and superposition: $\kappa \simeq v_s'' + v''$, where prime denotes derivation with respect to the spatial variable x_b.

Total elastic strain of the cable is given with the expression:

$$\varepsilon = \varepsilon_s + \left((1+u')^2 + (z'+w')^2 \right)^{1/2} - 1, \qquad (5)$$

_____

where ε_s is static strain and rest of the terms represent dynamic strain. The function $z(x_c)$ denotes function of the cable static equilibrium configuration and prime is derivation with respect to the spatial variable x_c.

The kinetic energy of the system is defined with:

$$T = \tfrac{1}{2}\int_0^l m_b \dot{v}^2 \, dx_b + \tfrac{1}{2}\int_0^L m_c \dot{u}^2 \, dx_c + \tfrac{1}{2}\int_0^L m_c \dot{w}^2 \, dx_c, \quad (6)$$

where dot represents derivation with respect to the time variable t.

After determining potential and kinetic energy variation, expressions are substituted into Hamilton's principle and the static equilibrium equations are taken into account. Then, the equations are separated by displacement components and the following equations of motion are obtained:

$$\left(E_c A_c \left(u' + z' w' \right) \right)' - m_c \ddot{u} = 0, \quad (7)$$

$$\left(E_c A_c \varepsilon_s w' + E_c A_c \left(z' + w' \right)\left(u' + z' w' \right) \right)' - m_c \ddot{w} = 0, \quad (8)$$

$$E_b I_b \, v^{IV} + m_b \ddot{v} = 0. \quad (9)$$

According to quasi-static stretching assumption [12], the longitudinal cable displacement defined by the equation (7) can be condensed. The expression (7) can directly be integrated after neglecting the inertia in longitudinal direction and by taking into account the boundary conditions:

$$u(0) = -v(0)\sin\varphi, \qquad u(L) = 0. \quad (10)$$

So, the stretching is defined by the expression:

$$e = \frac{v(0)\sin\varphi}{L} + \frac{1}{L}\int_0^L z' w' \, dx_c, \quad (11)$$

where $e=e(t)$ is the cable stretching. For low sag and high pretension force, it follows that $E_c A_c \varepsilon_s \approx H \sec\varphi$, where H represents horizontal component of the cable static tension. After condensation procedure, the equation (8) that defines cable transverse vibrations is:

$$m_c \ddot{w} - \left(H \sec\varphi \, w' + E_c A_c \left(z' + w' \right) e \right)' = 0. \quad (12)$$

By transforming the equations into dimensionless forms, the number of system parameters is reduced. Dimensionless relations of the variables and the system parameters are:

$$\tilde{w} = \frac{w}{L}; \; \tilde{x}_c = \frac{x_c}{L}; \; \tilde{z} = \frac{z}{L}; \; \tilde{v} = \frac{v}{l}; \; \tilde{x}_b = \frac{x_b}{l};$$

$$\eta = \frac{A_c E_c}{H \sec\varphi}; \; \upsilon = \frac{d}{L}; \; \chi = \frac{E_b I_b}{E_c A_c \, l^2}; \; \rho = \frac{m_c}{m_b}; \quad (13)$$

$$\mu = \frac{k \, l^3}{E_b I_b}; \; \bar{t} = \omega_1 t.$$

Time variable is transformed into dimensionless form by using first natural system frequency ω_1. The cable parameters are static elasticity measure η and sag to span ratio υ. Cable parameter η is inversely proportional to cable static stretching and its value mostly dependent on material elasticity. More elastic materials have smaller value of η, while for example steel cables, due to small deformation, have large parameter values ($\eta > 250$). Parameter υ defines cable geometry by describing depth of static profile. For $\upsilon < 1/8$, the parabolic assumption for the static profile can be used. Usually, this assumption greatly simplifies analytical analysis of the cable. The system parameter χ is ratio of beam and cable rigidity and ρ is cable and beam linear mass ratio. Both of these parameters greatly depend on material. It is intuitively clear that ρ should have small values, while value of χ is not only dependent on flexural stiffness of the beam and axial cable stiffness but also on the beam span. So, the analysis considers a wide interval for parameter χ values.

After transformation into dimensionless form, the equation (11) becomes:

$$\tilde{e} = \tilde{v}(0)\sin\varphi\cos\varphi + \int_0^1 \tilde{z}' \, \tilde{w}' \, d\tilde{x}_c. \quad (14)$$

Static profile of the low sag cable can be described by the parabola $\tilde{z}(\tilde{x}) = 4\upsilon\left(\tilde{x}_c - \tilde{x}_c^2 \right)$.

We neglect higher order terms in the equation (12) and transform equations of motion into the dimensionless form:

$$\frac{m_c L^2}{H \sec\varphi} \omega_1^2 \, \ddot{\tilde{w}} - \tilde{w}'' + 8\upsilon\eta\tilde{e} = 0, \quad (15)$$

$$\frac{m_b l^4}{E_b I_b}\omega_1^2 \ddot{\tilde{v}} + \tilde{v}^{IV} = 0. \tag{16}$$

Given equations need to satisfy following geometric and mechanical boundary conditions:

$$\tilde{w}(0) = \tilde{v}(0)\cos^2\varphi,$$
$$w(1) = 0,$$
$$\tilde{v}''(0) = 0,$$
$$\chi\,\tilde{v}'''(0) + \tilde{e}\sin\varphi - \frac{1}{\eta}\tilde{w}'(0)\cos\varphi - 4\upsilon\tilde{e}\cos\varphi = 0,$$
$$\tilde{v}_L\left(\tfrac{1}{2}\right) = \tilde{v}_R\left(\tfrac{1}{2}\right),$$
$$\tilde{v}_L'\left(\tfrac{1}{2}\right) = \tilde{v}_R'\left(\tfrac{1}{2}\right), \tag{17}$$
$$\tilde{v}_L''\left(\tfrac{1}{2}\right) = \tilde{v}_R''\left(\tfrac{1}{2}\right),$$
$$\tilde{v}_L'''\left(\tfrac{1}{2}\right) - \mu\tilde{v}_L\left(\tfrac{1}{2}\right) - \tilde{v}_R'''\left(\tfrac{1}{2}\right) = 0,$$
$$\tilde{v}(1) = 0,$$
$$\tilde{v}'(1) = 0.$$

$\tilde{v}_L$ and $\tilde{v}_R$ denote left and right function $v(x_b,t)$ values to the elastic spring in the middle of the beam span.

2.2 Derivation of characteristic equation

The solution of equations (15) and (16) is obtained by separating variables:

$$\tilde{w}(\tilde{x}_c,\bar{t}) = \phi(\tilde{x}_c)\exp(i\tfrac{\omega}{\omega_1}\bar{t}),$$
$$\tilde{v}(\tilde{x}_b,\bar{t}) = \psi(\tilde{x}_b)\exp(i\tfrac{\omega}{\omega_1}\bar{t}). \tag{18}$$

Whereupon the following equations are obtained:

$$\beta_c^2\phi + \phi'' = 8\upsilon\eta\bar{e}, \tag{19}$$

$$\beta_b^4\psi - \psi^{IV} = 0, \tag{20}$$

where:

$$\beta_c^2 = \omega^2\frac{m_c L^2}{H\sec\varphi}, \quad \beta_b^4 = \omega^2\frac{m_b l^4}{E_b I_b}, \tag{21}$$

$$\bar{e} = \psi_1(0)\sin\varphi\cos\varphi + \int_0^1 4\upsilon(1-2\tilde{x}_c)\phi'(\tilde{x}_c)d\tilde{x}_c. \tag{22}$$

The function describing the mode shape of the beam is defined as $\psi(\tilde{x}_b) = \psi_1(\tilde{x}_b)\cup\psi_2(\tilde{x}_b)$. The function $\psi_1(\tilde{x}_b)$ is defined on the interval $\tilde{x}_b \in \left(0,\tfrac{1}{2}\right)$ and $\psi_2(\tilde{x}_b)$ is defined on the interval $\tilde{x}_b \in \left(\tfrac{1}{2},1\right)$. Functions $\phi(\tilde{x}_c)$, $\psi_1(\tilde{x}_b)$, and $\psi_2(\tilde{x}_b)$ need to fulfill boundary conditions (17). This procedure is performed using Wolfram *Mathematica* program and the following equation is obtained:

$$\begin{aligned}
&\frac{\beta_c\cos^3\varphi\cot\beta_c}{\eta} - \frac{\hat{e}\left(4\upsilon\cos\varphi\left(\beta_c - 2\tan\tfrac{\beta_c}{2}\right) - \beta_c\sin\varphi\right)}{\beta_c} \\
&\quad + \frac{\beta_b^3\chi\left(1+\cos\beta_b\cosh\beta_b\right)}{\cosh\beta_b\sin\beta_b - \cos\beta_b\sinh\beta_b} \\
&\quad + \frac{\mu\chi\left(\sin\beta_b\left(1+\cosh\beta_b\right) - \sinh\beta_b\left(1+\cos\beta_b\right)\right)}{4\cosh\beta_b\sin\beta_b - 4\cos\beta_b\sinh\beta_b} \\
&\quad + \frac{\mu\left(\cosh\beta_b - \cos\beta_b + 4\sin\tfrac{\beta_b}{2}\sinh\tfrac{\beta_b}{2} - 2\sin\beta_b\sinh\beta_b\right)}{4\beta_b^3\left(\cosh\beta_b\sin\beta_b - \cos\beta_b\sinh\beta_b\right)} \\
&\quad \cdot\left[\frac{\beta_c\cos^3\varphi\cot\beta_c}{\eta} - \frac{\hat{e}\left(4\upsilon\cos\varphi\left(\beta_c - 2\tan\tfrac{\beta_c}{2}\right) - \beta_c\sin\varphi\right)}{\beta_c}\right] = 0,
\end{aligned} \tag{23}$$

where:

$$\beta_c = \frac{\beta_b^2\sqrt{\eta\rho\chi}}{\cos\varphi}, \tag{24}$$

$$\hat{e} = \frac{\beta_c^2\cos\varphi\left(\beta_c\sin\varphi - 4\upsilon\cos\varphi\left(\beta_c - 2\tan\tfrac{\beta_c}{2}\right)\right)}{\beta_c^3 - \beta_c\lambda^2 + 2\lambda^2\tan\tfrac{\beta_c}{2}}. \tag{25}$$

The equation (23) is analogous to the solution derived by Gattulli [9] if we set $\mu=0$:

$$\begin{aligned}
&\frac{\beta_c\cos^3\varphi\cot\beta_c}{\eta} - \frac{\hat{e}\left(4\upsilon\cos\varphi\left(\beta_c - 2\tan\tfrac{\beta_c}{2}\right) - \beta_c\sin\varphi\right)}{\beta_c} \\
&\quad + \frac{\beta_b^3\chi\left(1+\cos\beta_b\cosh\beta_b\right)}{\cosh\beta_b\sin\beta_b - \cos\beta_b\sinh\beta_b} = 0.
\end{aligned} \tag{26}$$

If the beam is not elastically supported, its deformation is defined using only one function $\psi(\tilde{x}_b) = \psi_1(\tilde{x}_b)$. In that case, mode shape analytical functions are given by the following expressions:

$$\phi(\tilde{x}_c) = A_1 \frac{16\eta\upsilon\hat{e}}{\beta_c^2}\left(1 - \cos(\beta_c\tilde{x}_c) - \tan\frac{\beta_c}{2}\sin\beta_c\tilde{x}_c\right)$$

$$+ 2A_1\cos^2\varphi\left(\cos(\beta_c\tilde{x}_c) - \cot\beta_c\sin(\beta_c\tilde{x}_c)\right),$$

$$\psi(\tilde{x}_b) = A_1\cos(\beta_b\tilde{x}_b) + A_1\cosh(\beta_b\tilde{x}_b) \tag{27}$$

$$- A_1\left(\frac{1 + \cos\beta_b\cosh\beta_b + \sin\beta_b\sinh\beta_b}{\cosh\beta_b\sin\beta_b - \cos\beta_b\sinh\beta_b}\right)\sin(\beta_b\tilde{x}_b)$$

$$- A_1\left(\frac{\cos\beta_b\coth\beta_b + \operatorname{csch}\beta_b - \sin\beta_b}{\cos\beta_b - \coth\beta_b\sin\beta_b}\right)\sinh(\beta_b\tilde{x}_b),$$

where constant $A_1 = \psi(0)/2$ depends on the shape function normalization.

3   Analysis of the results

For the parametric analysis of system dynamic properties, fixed values are given to the parameters η, υ and ρ, while the parameter χ is varied to obtain different values for β_c and β_b. We consider two cable-stayed models. The beam of the model A is not supported by the elastic spring ($\mu=0$) and eigenvalue equation is defined by the expression (26), while the beam of the model B is supported by the elastic spring ($\mu\neq0$) and corresponding frequency equation is defined by the expression (23). In all models, the angle of cable to the beam is given by geometric relation $\tan\varphi=1/2$. Solution of

the equations (23) and (26) is determined numerically by Wolfram *Mathematica*.

3.1 Model A results

For cable parameters $\eta=800$ and $\upsilon=5\cdot10^{-4}$, eigenvalues β_c and β_b for the first six modes are determined and displayed in Fig. 2. For dynamic properties analysis only upper spectrum which shows the cable eigenvalues β_c can be used. The eigenvalue β_c is proportional to system frequency ω as given in the expression (21). The ratio of eigenvalues β_c corresponds to the ratio of system frequencies, so β_c can be considered as dimensionless system frequency. The relation of β_b with ω and β_c that is given by the expressions (21) and (24) is not linear, so it was not used in the result analysis. In the Fig. 2 can be noticed the eigenvalues $\beta_c\approx n\pi$, for $n=1,2,3…$ These eigenvalues are well known taut cable dimensionless frequencies [12]. Figure 3 displays system shape functions and three types of modes can be identified. First mode is *global* and mainly involves deformation of the beam while the cable behaves as tendon. Second, fourth and sixth mode are *local* cable modes, while third and fifth modes are *hybrid* because the beam and the cable are involved in the motion.
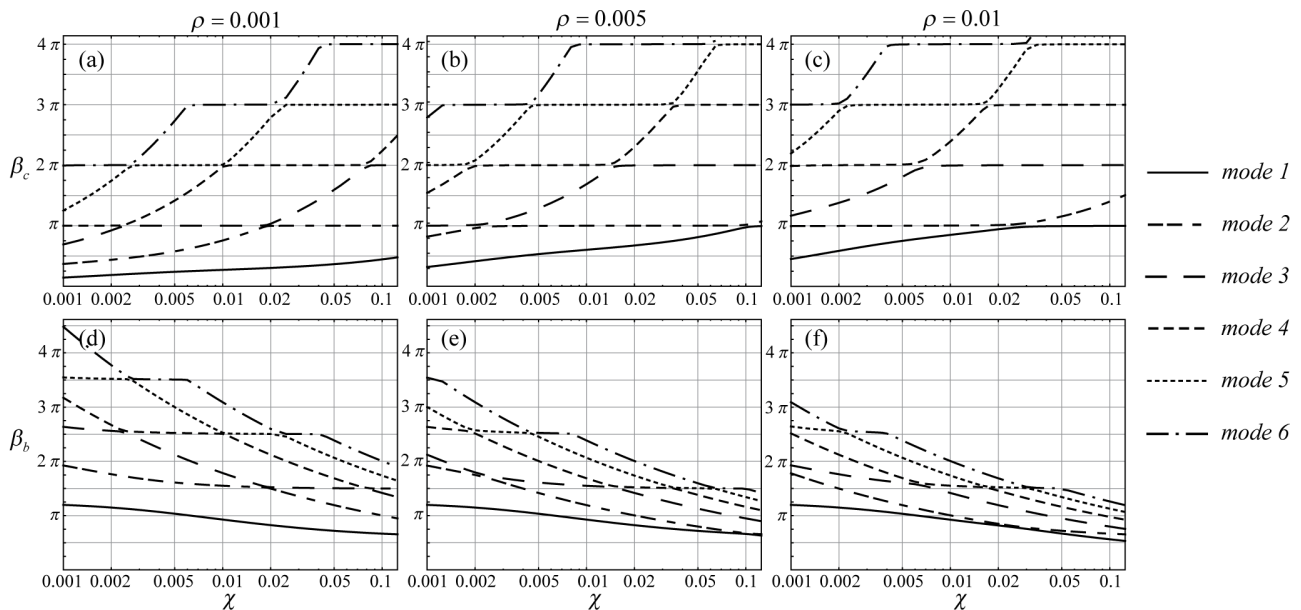

Figure 2. Model A eigenvalues spectra for parameters $\eta=800$ and $\upsilon=5\cdot10^{-4}$: β_c (a,b,c); β_b (d,e,f).

System frequency values are increased with an increase in ρ and χ parameters, which can be seen on β_c spectra. For $\rho=0.001$, Fig. 2(a) shows that for very low χ values ($\chi<0.002$), the beam is very flexible and in low order modes cable acts as tendon or a flexible support of the beam. The change between local cable and system modes happens for $\chi\approx0.0025$ and $\chi\approx0.019$. With an increase in the parameter χ value, the beam is stiffer and frequencies of modes including notable beam deformation are higher. This kind of behavior can be observed for all constant values of ρ. The influence of the parameter ρ can be observed in adjacent β_c spectra displayed in Fig. 2 (a) – (c). Also, in this case, smaller value of the parameter indicates the system having a more flexible beam.

For parameter values $\eta=800$, $\upsilon=5\cdot10^{-4}$, $\rho=5\cdot10^{-3}$ and $\chi=3.75\cdot10^{-3}$ (Fig. 3), frequency ratio between global and local mode is $\omega_1\approx\omega_2/2$. In this case, cable oscillations can be induced by beam through angle-variation mechanism [10]. The same type of resonance is possible between third (hybrid) and fifth (local) mode for parameter values $\eta=800$, $\upsilon=5\cdot10^{-4}$, $\rho=5\cdot10^{-3}$ and $\chi=7.5\cdot10^{-3}$ (Fig. 4). Parameter values for which the system frequencies meet one-to-one internal resonance condition can easily be identified in the β_c spectrum because there is veering of the system frequencies values.
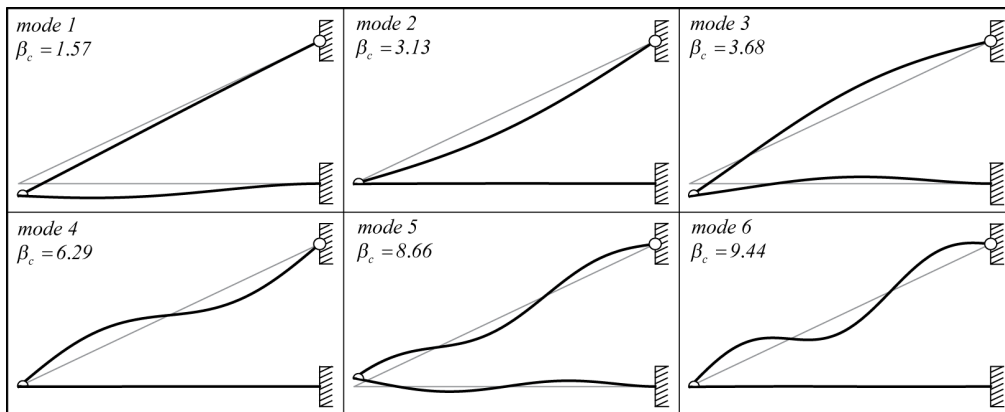

Figure 3. Model A mode shapes for parameters $\eta=800$, $\upsilon=5\cdot10^{-4}$, $\rho=5\cdot10^{-3}$ and $\chi=3.75\cdot10^{-3}$.
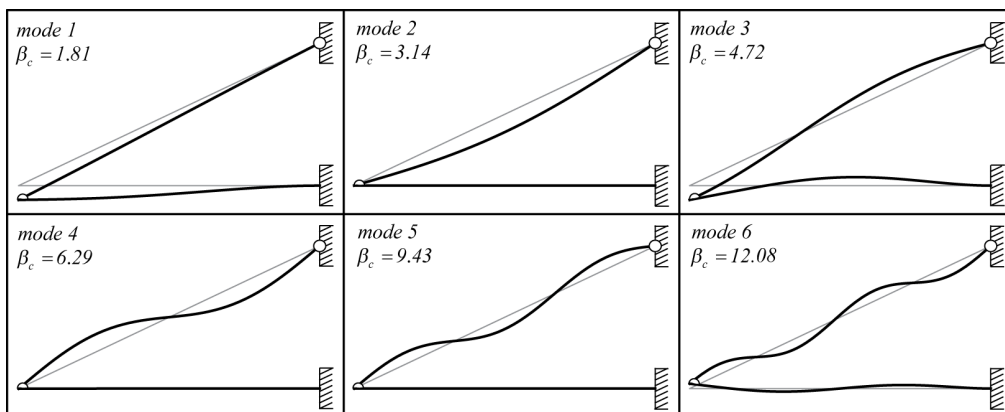

Figure 4. Model A mode shapes for parameters $\eta=800$, $\upsilon=5\cdot10^{-4}$, $\rho=5\cdot10^{-3}$ and $\chi=7.5\cdot10^{-3}$.
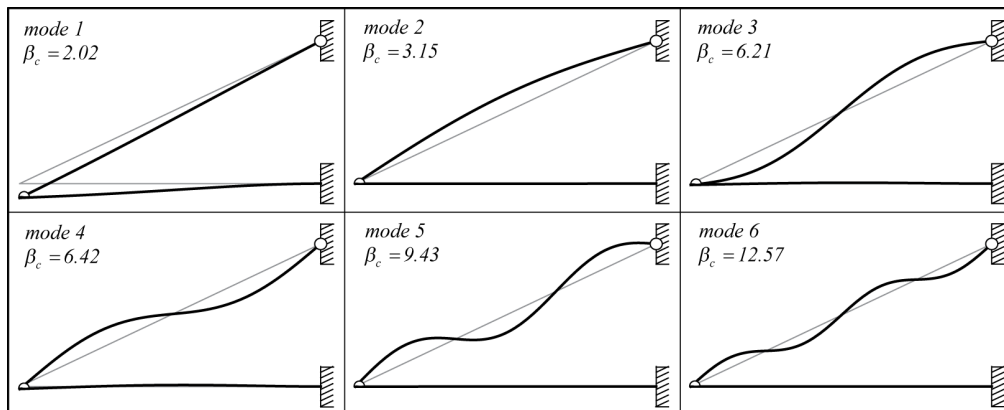
Figure 5. Model A mode shapes for parameters $\eta=800$, $\upsilon=5\cdot10^{-4}$, $\rho=5\cdot10^{-3}$ and $\chi=1.5\cdot10^{-2}$.

Table 1. Model A natural frequencies for $\eta=800$, $\upsilon=5\cdot10^{-4}$ and $\rho=5\cdot10^{-3}$

		ω_1	ω_2	ω_3	ω_4	ω_5	ω_6
$\chi=3.75\cdot10^{-3}$	Analytic	21.93	43.90	51.53	88.03	121.31	132.20
	SAP	21.76	44.02	51.25	87.99	117.78	131.39
$\chi=7.5\cdot10^{-3}$	Analytic	25.31	44.02	66.05	88.13	132.02	169.24
	SAP	25.26	43.98	64.96	87.77	130.81	164.52
$\chi=1.5\cdot10^{-2}$	Analytic	28.33	44.06	86.97	89.91	132.07	176.04
	SAP	28.23	43.95	86.01	88.75	130.65	172.87

There can be also noted that for certain values of the parameters, a necessary condition for multiple-resonance is also fulfilled. By comparing the ratio of β_c values of modes displayed in Fig. 5, it follows that system meets the requirements for 1:1 internal resonance of third and fourth mode, and auto-parametric resonance 1:2 between third/forth mode and second system mode. Commercial software package CSI SAP2000 v15 was used to form finite element model of the system. In finite element model, the following physical parameters were selected: beam length $l=10$ [m], axial stiffness of cable $A_cE_c=1.6\cdot10^5$ [kN] and cable mass $m_c=8.15$ [kg/m′]. Flexural stiffness and mass of the beam are selected to obtain dimensionless parameters ρ and χ values. The cable is modeled using 20 *cable elements*. To fit the cable parameters $\upsilon=5\cdot10^{-4}$ and $\eta=800$, nonlinear static analysis is performed to obtain cable target force $T\approx200$ [kN]. After obtaining nonlinear static equilibrium configuration, dynamic properties are determined, i.e., frequencies

and mode shapes. Mode shapes displayed in Figs. 3–5 correspond to those determined by the finite element model. Frequencies values for assigned physical parameters in model A are given in Table 1. The finite element model results show a very good correspondence with the analytic model.

The eigenvalue β_c spectra for other taut cable parameter values are displayed in Fig. 6. Spectra displayed in Fig. 6 (a) – (c) show that smaller value of cable parameter η induces more global and hybrid modes in low order system modes. This is because the elastic pretension of cable significantly contributes to overall structural stiffness. Spectrum displayed in Fig. 6 (d) – (f) shows the system with larger value of cable sag to span ratio υ. The cable sag influences cable symmetric modes so that their frequency has a higher value [12]. The spectra are very similar to those shown in Fig. 2, but for higher values of mass ratio, the veering region of the low-order system modes is wider.
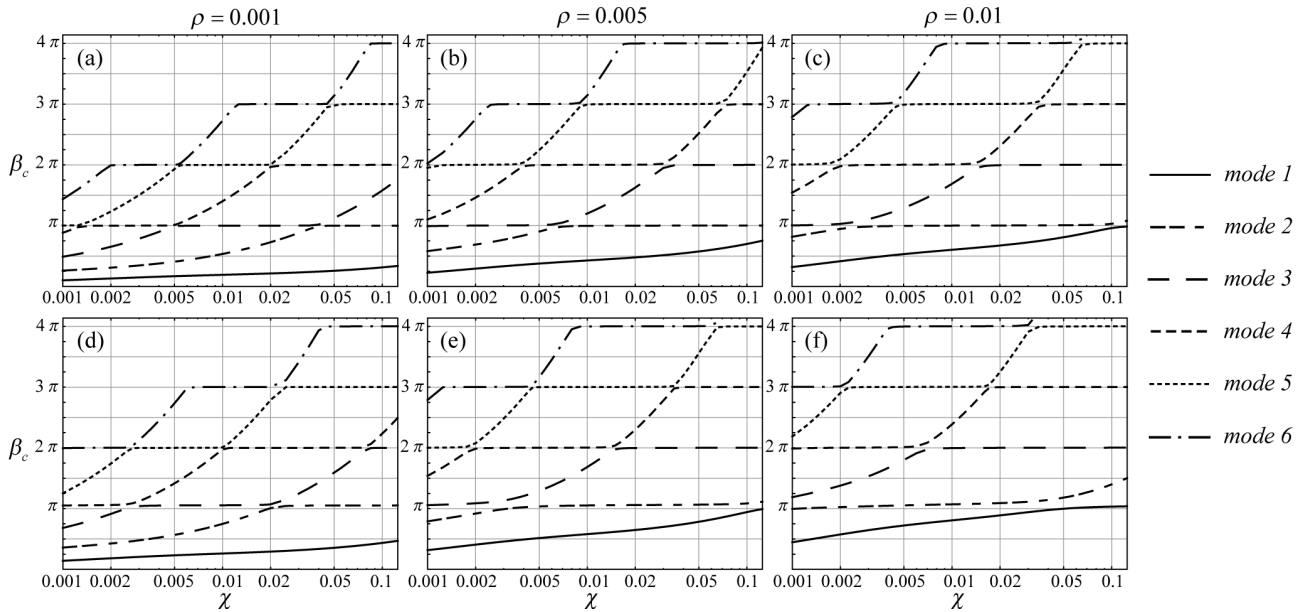
_____

Figure 6. Model A eigenvalues β_c spectra: $\eta=400$ and $\upsilon=5 \cdot 10^{-4}$ (a,b,c); $\eta=800$ and $\upsilon=5 \cdot 10^{-3}$ (d,e,f).

3.2 Model B results

The system rigidity in a model B is influenced by elastic spring stiffness related to the axial tendon stiffness value. By assuming that the cable and tendon have the same axial stiffness, i.e., $E_tA_t=E_cA_c$, the parameter μ is:

$$\mu = \frac{2\cos\gamma\sin^2\gamma}{\chi}. \qquad (28)$$

The same system parameter values as the ones of the model A are considered. Spectra for eigenvalues β_c are displayed in Fig. 7. Integer frequency ratios, which are similar to the previous examples, can be easily identified on the spectra. It can be noted that elastic support of the beam influences dynamic properties by increased frequency values of global and hybrid modes. Eigenvalues spectra of models A and B are almost without change for mass ratio $\rho=0.001$. A slightly higher eigenvalue can be noticed only for low order global modes. Significantly larger eigenvalues of the global and hybrid modes in model B exist for higher mass ratio ρ. This is because more local cable modes occur in low-order system modes.

Particularly interesting is the spectra for $\rho=0.01$ and $\eta=800$ displayed in Fig. 7(c) because continuous veering of the first and the second mode happens. It

means that such a system satisfies one-to-one internal resonance condition of low-order modes in wide range of the parameter χ values. In the case of smaller cable sag $\upsilon=5 \cdot 10^{-3}$, Fig. 7(i) shows that eigenvalues of the first and the second mode are very close in broad interval of parameter χ values.

Also, these modes have very similar mode shapes that are displayed in Fig. 8. Veering region modes involve coupled motion of the cable and the beam with considerably larger cable displacements.

It can be pointed out that shape functions with eigenvalue $\beta_c < \pi$ but also not too close to π, are global and the cable behaves as a tendon, which can be seen in Fig. 9. For eigenvalues $\beta_c \geq \pi$, all modes are either local or coupled beam-cable motion. Hybrid modes that are close to local cable modes involve very small displacements of the beam and large displacements of the cable. While for well separated frequencies, hybrid mode shapes can be classified as global because the beam and the cable displacement are of the same order.

To verify the replacement of the tendon with the spring, two finite element models are formed. One system is modeled with the spring having equivalent stiffness given by expression (2) and the other with massless tendon element. As the beam is additionally supported in the middle of the span, its length is $l=20$ [m], while cable stiffness is the same as in the model A. Cable target force and mass are selected to fit different values to the cable
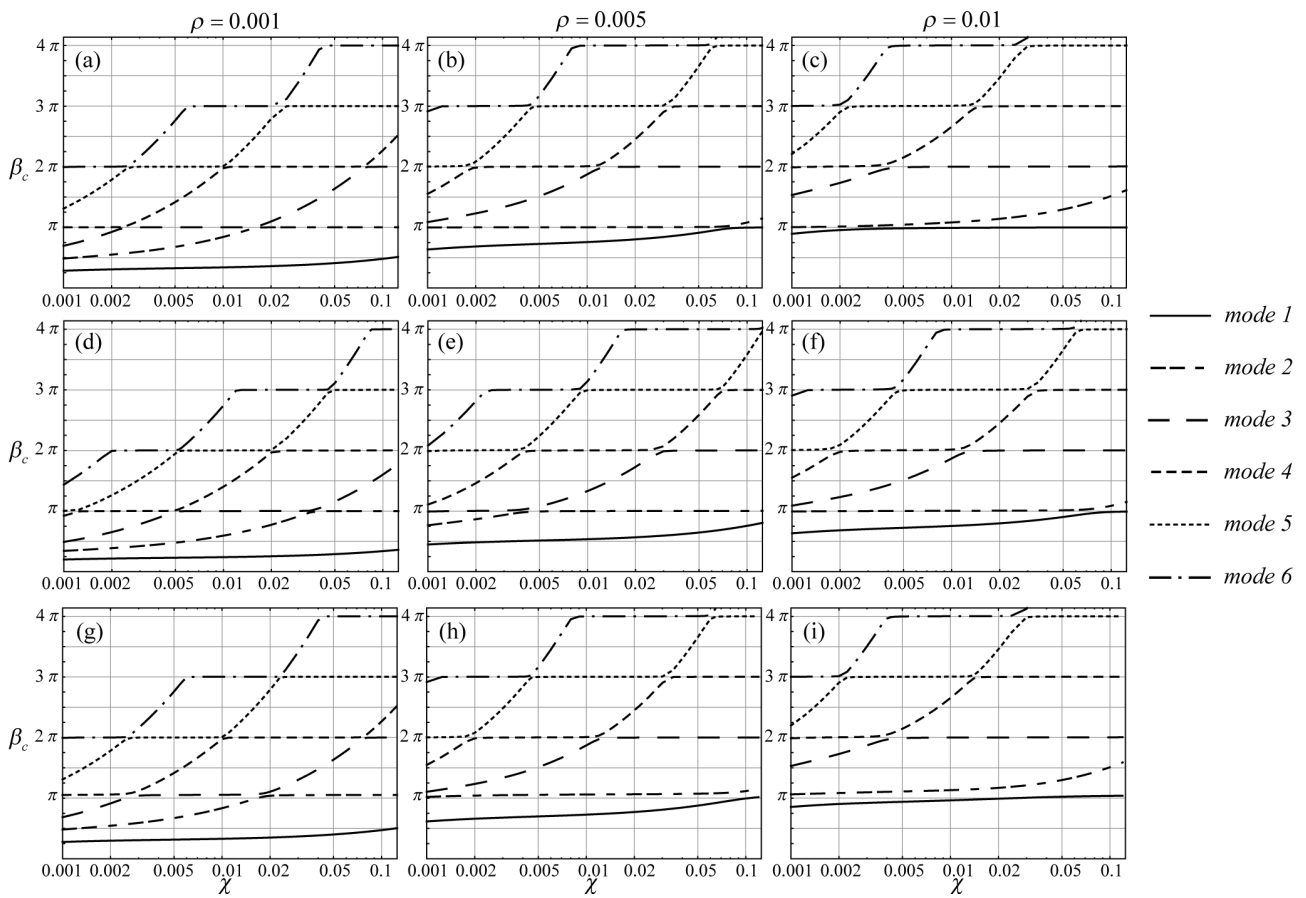
Figure 7. Model B eigenvalues β_c spectra: $\eta=800$ and $\upsilon=5\cdot10^{-4}$ (a,b,c); $\eta=400$ and $\upsilon=5\cdot10^{-4}$ (d,e,f); $\eta=800$ and $\upsilon=5\cdot10^{-3}$ (g,h,i).
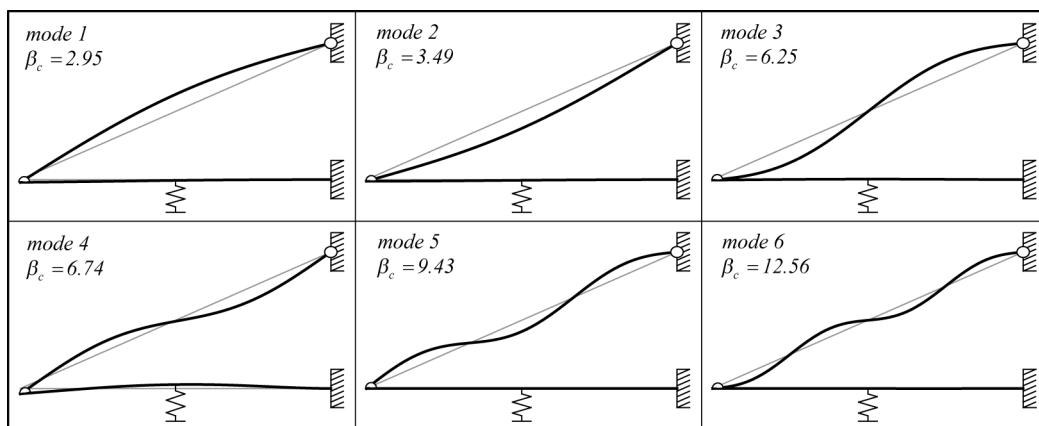

Figure 8. Model B mode shapes for parameters $\eta=800$, $\upsilon=5\cdot10^{-3}$, $\rho=10^{-2}$ and $\chi=5\cdot10^{-3}$.
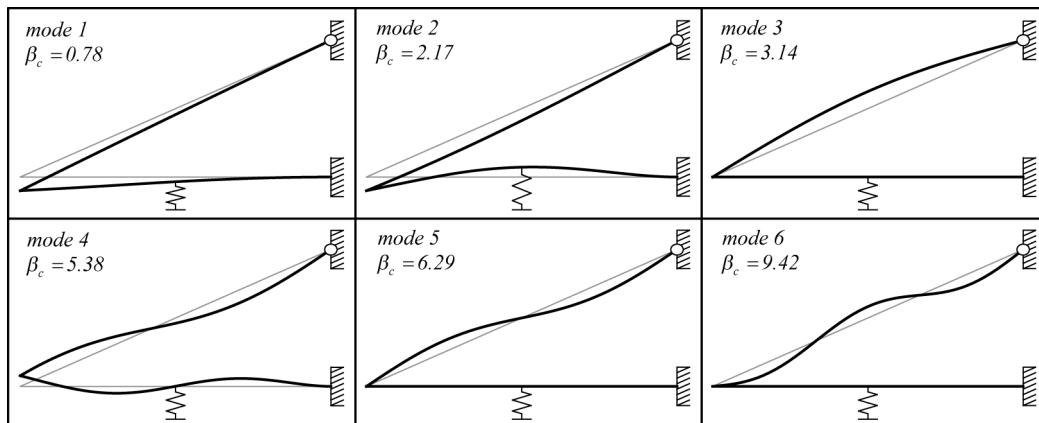
Figure 9. Model B mode shapes for parameters $\eta=400$, $\upsilon=5\cdot10^{-4}$, $\rho=10^{-3}$ and $\chi=1.5\cdot10^{-2}$.

Table 2. Model B natural frequencies for $\eta=800$

		ω_1	ω_2	ω_3	ω_4	ω_5	ω_6
$\upsilon=5\cdot10^{-3}$	Analytic	9.24	10.92	19.58	21.11	29.54	39.33
$\rho=0.01$	SAP-spring	9.31	10.99	19.38	21.01	29.28	38.46
$\chi=5\cdot10^{-3}$	SAP-tendon	9.30	10.98	19.38	20.98	29.28	38.45
$\upsilon=5\cdot10^{-4}$	Analytic	7.71	21.49	31.14	53.23	62.25	93.33
$\rho=1\cdot10^{-3}$	SAP-spring	7.83	21.38	30.87	52.82	61.54	91.83
$\chi=1.5\cdot10^{-2}$	SAP-tendon	7.82	21.36	31.15	52.76	61.53	92.57

parameters η and υ, and beam properties are adopted to obtain the parameter values ρ and χ given in Figs. 8 and 9.

Table 2 shows the frequency values for all models and there is very good agreement of the analytical results with both finite element models. Mode shapes of finite element model correspond to those shown in Figs. 8 and 9.

4   Conclusion

The parametric analysis of cable-stayed system dynamic properties using eigenvalue spectra and mode shapes showed several interesting features. The system has global beam-tendon behavior for the eigenvalue $\beta_c < \pi$. Mode shapes that have larger eigenvalues are either local cable modes or hybrid involving coupled cable-beam motion. Analysis of eigenvalue spectra showed that integer frequency ratio condition exists for various system parameters and system dynamic response could lead to potential internal resonances and/or auto-parametric resonance. Also, for certain parameter values, conditions for multiple resonances are fulfilled.

Finite element models verified the results obtained by analytical modeling.

Analysis of dynamic properties showed that motion of the beam and cable could be highly coupled in a certain frequency range. Therefore, the models in which cables are treated solely as tendon members may be inadequate. The significance of presented analytical model is that it allows simple and fast analysis of frequency variation correlated with dimensionless system parameters. Also, the integer frequency ratio can easily be noticed on eigenvalue spectra. Engineering requirements for cable stayed system properties (cable stays in [11]) recommended that system frequency values should be well separated from local cable frequencies, which is sometimes hard to achieve, especially for various integer frequency ratios. The presented model could be used for further study of cable-beam interaction caused by dynamic excitations in order to evaluate frequency ratios that could be particularly unfavorable in real structures.

References

[1] Luo, J., Liu, X.: *An approximate response of the large system with local cubic nonlinearities subjected the harmonic excitation*, Engineering Review, 35 (2015), 1, 49-59.

[2] Srinil, N., Rega, G., Chucheepsakul, S.: *Three-dimensional non-linear coupling and dynamic tension in the large-amplitude free vibrations of an sagged cables*, Journal of Sound and Vibration, 269 (2004), 823-852.

[3] Perkins, N.C.: *Modal interactions in the non-linear response of elastic cables under parametric/external excitation*, International Journal of Nonlinear Mechanics, 27 (1992)**,** 2.

[4] Lilien, J. L., Pinto da Costa, A.: *Vibration amplitudes caused by parametric excitation of cable stayed structures*, Journal of Sound and Vibration, 174 (1994), 69-90.

[5] Demšić, M., Raduka, V.: *Oscilacije kabela uslijed indirektne pobude*, Građevinar, 67 (2015), 9, 829-841.

[6] Douthe, C. E., Gantes, C. J.: *Investigation of coupling between external and parametric resonances in small sagged inclined cables*, 3rd International Conference on Computational Methods in Structural Dynamics and Earthquake Engineering, Corfu, Greece, 2011.

[7] Caetano, E., Cunha A.: *Experimental analysis of coupled cable-deck motions in cable-stayed bridges*, 11th world conference on Earthquake Engineering, Acapulco, Mexico, 1996.

[8] Lin, K., Zou, D., Wei, M.: *Nonlinear analysis of cable vibration of a multispan cable-stayed bridge under transverse excitation*, Mathematical Problems in Engineering, Volume 2014, Article ID 832432.

[9] Gattulli, V., Morandini, M., Paolone, A.: *A parametric analytical model for non-linear dynamics in cable-stayed beam*, Earthquake Engineering and Structural Dynamics, 31 (2002), 1281-1300.

[10] Gattulli, V., Lepidi, M.: *Nonlinear interactions in the planar dynamics of cable-stayed beam*, International Journal of Solids and Structures, 40 (2003), 4729-4748.

[11] SETRA. *Cable stays*: *Recommendation of French Interministerial Commission on prestressing*, Center des Techniques des Ouvrages d'Art, Bagneux Cedex, France, 2002.

[12] Irvine, H. M.: *Cable structures*. The MIT Press, Cambridge, Massachusetts, 1981.